Investigation of the magnetic field influence on the plasma parameters homogeneity in a large H^- / D^- RF ion source relevant for ITER

L. Schiesko, P. Franzen, and U. Fantz

Max-Planck-Institut für Plasmaphysik, EURATOM Association, Boltzmannstrasse 2, D-85748 Garching, Germany

E-mail: loic.schiesko@ipp.mpg.de

Abstract. A study was conducted on the large 1/2-size ITER source RADI testbed in order to determine the influence of the magnetic field strength on the plasma parameters in the neighbourhood of the grid. The magnetic field at RADI is created by a current flowing in the plasma grid; in contrast to the small IPP prototype source where permanent magnets are used. The investigations show a plasma homogeneity within 10 % near the grid along the direction of the magnetic field lines as well as a reduction of the electron temperature. In the direction perpendicular to the magnetic field lines, and for field strengths higher than 2.4 mT, the density shows a minimum due to the reduced transport coefficient across a perpendicular magnetic field. A form of effective enhanced confinment is achieved for low magnetic field intensity.

1. Introduction

The development of powerful negative hydrogen ion sources for the ITER neutral beam heating system has been ongoing at IPP for several years [1, 2]. Currently, a new testbed, ELISE [3] is under construction. The ELISE testbed will hold a "half-size" ITER source and is an intermediate step between the currently operated sources and the full ITER size source. The sources of the RADI [4, 5] and ELISE testbeds are equipped with four drivers in a 2 x 2 arrangement and are of a comparable size ($0.8 \times 0.76\,m^2$ for RADI and $1 \times 0.86\,m^2$ for ELISE). On the RADI testbed where no extraction of the negative ions is possible due to hardware restrictions, a "dummy grid" (DG) is installed. It has the same conductance as an extraction system.
On the other IPP testbeds, MANITU [6, 7] and BATMAN [8, 9] the source is smaller ($0.32 \times 0.59\,m^2$, each) and equipped with only one driver. On these smaller sources the magnetic field is generated near the plasma grid by permanent magnets. The purpose of the filter field is to reduce the electron temperature below 2 eV to reduce the destruction of the negative ions by electron collisions. Moreover, the magnetic field reduces the amount of co-extracted electrons and enhances the extraction probability of the negative ions. The use of permanent magnets on RADI, ELISE and for the ITER-like

source SPIDER and MITICA [10, 11], due to the larger size of the source, would result in a weak magnetic field strength in front of the grid [4]. For this reason the field is generated instead by a current flowing through the grid. On the smaller testbed BATMAN, cross-B drifts due to the presence of the magnetic field are observed [8, 12] and it could be shown that they were dependant of the strength of the magnetic field [12]. Typically these drifts lead to assymetries in the plasma parameters (see [12]) and especially assymetric positive ion and electron densities. How these assymmetries will affect the negative ion generation on the grid and if the beam homogeneity will be affected are still open issues under investigation. Initial results showed a dependance of beam homogeneity with the plasma homogeneity in front of the grid [13], but the latest study performed with an improved database showed almost no correlation [14]. Nevertheless, in order to obtain an homogeneous extracted negative ion beam, an homogeneous grid illumination by the plasma can only be helpful.

Several attempts have been made to model the different aspects of the small sources [15, 16, 17, 18, 19]. All these codes are 2D except the one of Mochalskyy [18] which is fully 3D but limited to the neighbourhood of a hole of the PG. The results of all these simulations give some insights of the physics involved in the source. However, the complexity of the magnetic field configuration, combined with the high injected RF power requires a full 3D modeling of the source in order to understand the underlying mechanisms in detail. Two main issues are, for the moment, hampering the 3D modeling. First, is that the high density of the plasma (from 10^{17} to $10^{18}\,\mathrm{m}^{-3}$) and the large source size requires computing power greatly exceeding the commonly available cluster capacities. Second, that the boundary conditions of the walls are, at present, not satisfactorily defined for a 3D environment.

To our knowledge, at the moment, no attempt to model large sources like RADI is underway. As the magnetic field configuration between the large and small test beds are very different the results obtained by the simulations for the small test beds will probably differ from what is measured at RADI.

As drifts were observed in the other sources, it was anticipated they would be also seen at RADI. One of the goals of this paper is to compare their influence on RADI with what was already observed at BATMAN. Further goal is to determine the influence of the magnetic field on the homogneity of the plasma parameters in front of the grid. To accomplish this, two movable Langmuir probes, located in a distance of 2 cm from the dummy grid were used. In the following section the RADI testbed, the Langmuir probes and the analysis system are described. Lastly, the homogeneity of the plasma in the vicinity of the dummy grid will be discussed.

2. Experimental setup and data evaluation

The source of RADI [4, 5] is a scaling of the IPP prototype source with four drivers in a 2 x 2 arrangement. The Langmuir probes can be seen on figure 1. The plasma

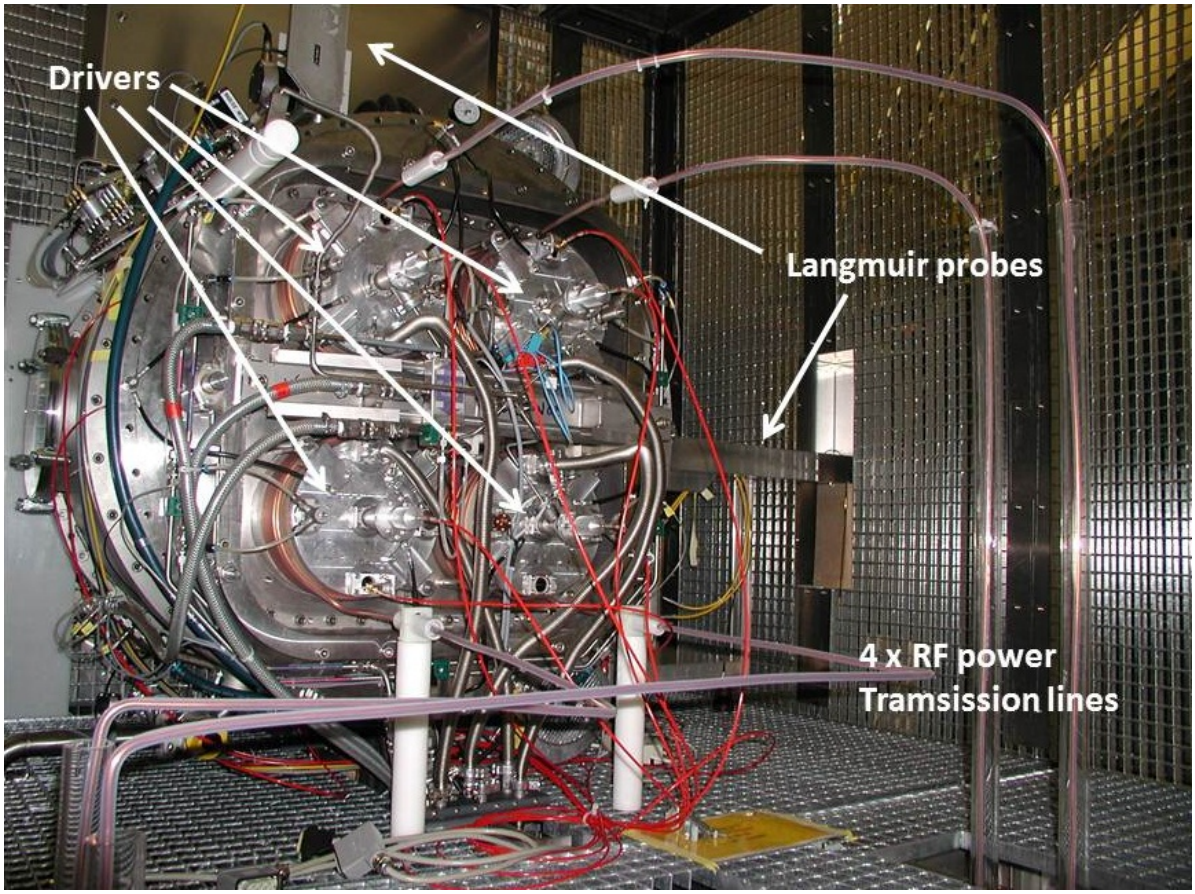

Figure 1. Picture of the RADI testbed.

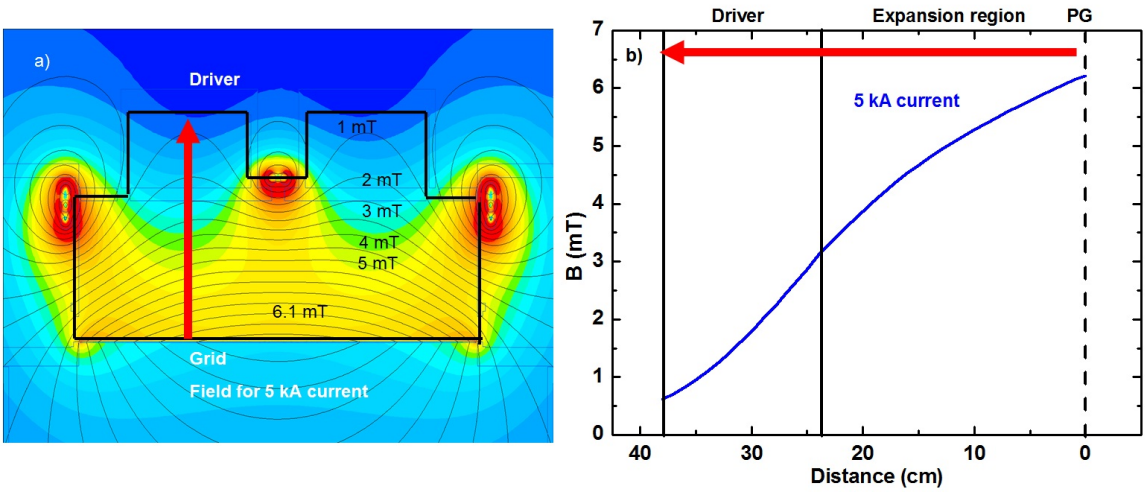

Figure 2. a) presents a 2D map of the magnetic field obtained for injected current of 5 kA, while b) is the variation of the horizontal field strength along the arrow of a).

is generated by two generators (P_{max} = 180 kW, f = 1 MHz), with each connected to two drivers. The experiments were conducted in hydrogen and deuterium plasmas, at a discharge pressure of 0.6 Pa and 160 kW of total injected RF power (40 kW per driver).

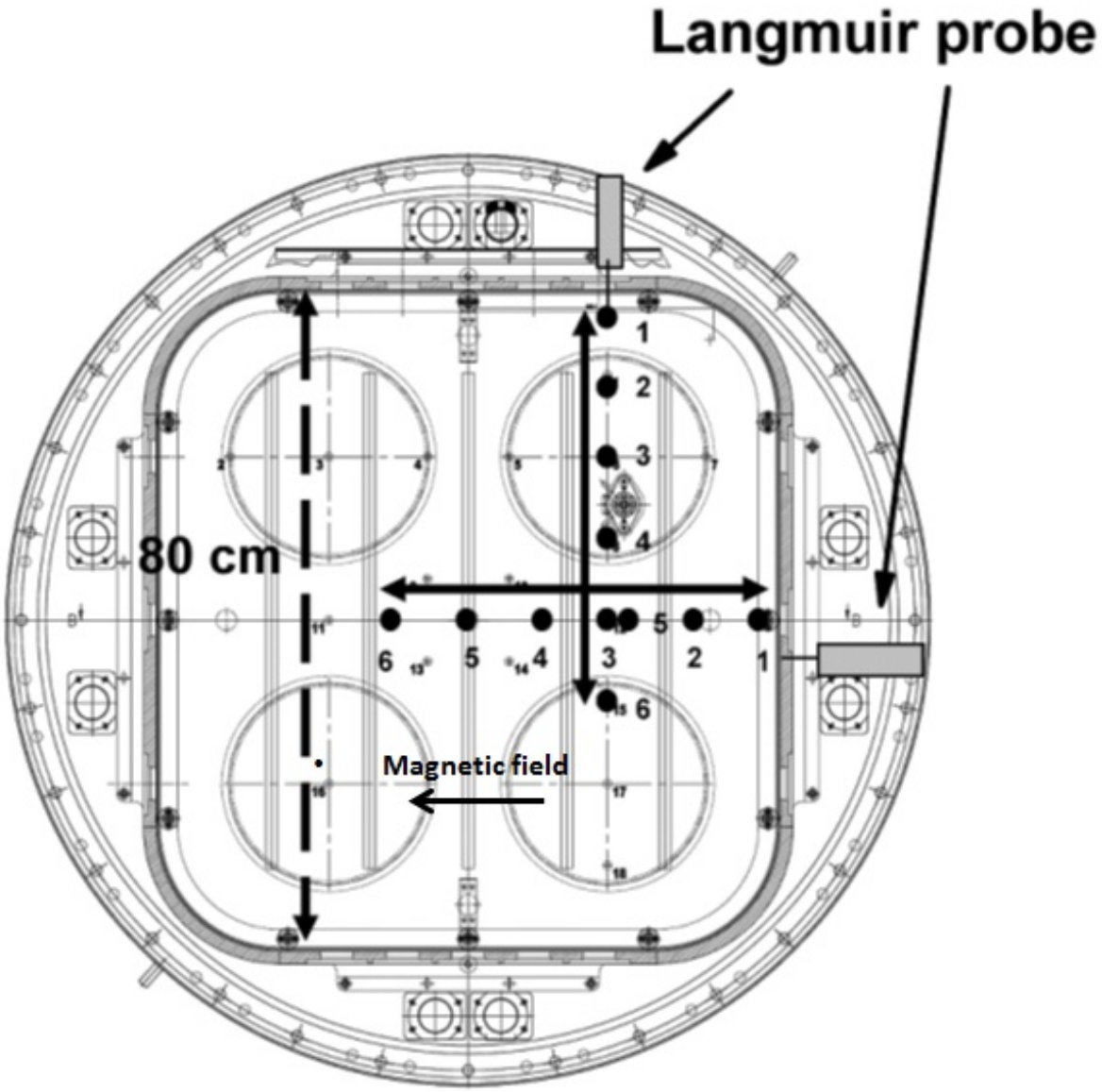

Figure 3. Schematic representation of the Langmuir probes locations and measurement points. The projection of the drivers and the grid slits as well as the magnetic field lines direction is also indicated.

The pressure of 0.6 Pa was chosen in order to compare the results from RADI with those from the smaller ion source on the testbed BATMAN. At the smaller testbeds with the new magnetic frame it is not possible to sustain the plasma at the ITER relevant pressure of 0.3 Pa [12] ‡. At the small prototype source, this correlates with the magnetic field lines penetrating the driver combined with a strong neutral depletion because of the high injected RF power [21]. This problem of source operating pressure was; how-

‡ The purpose of this new frame installed on the small test beds was to test different magnetic field configurations in order to optimize the source performance. With the standart magnetic field configuration, the small sources could be operated at a low pressure of 0.3 Pa.

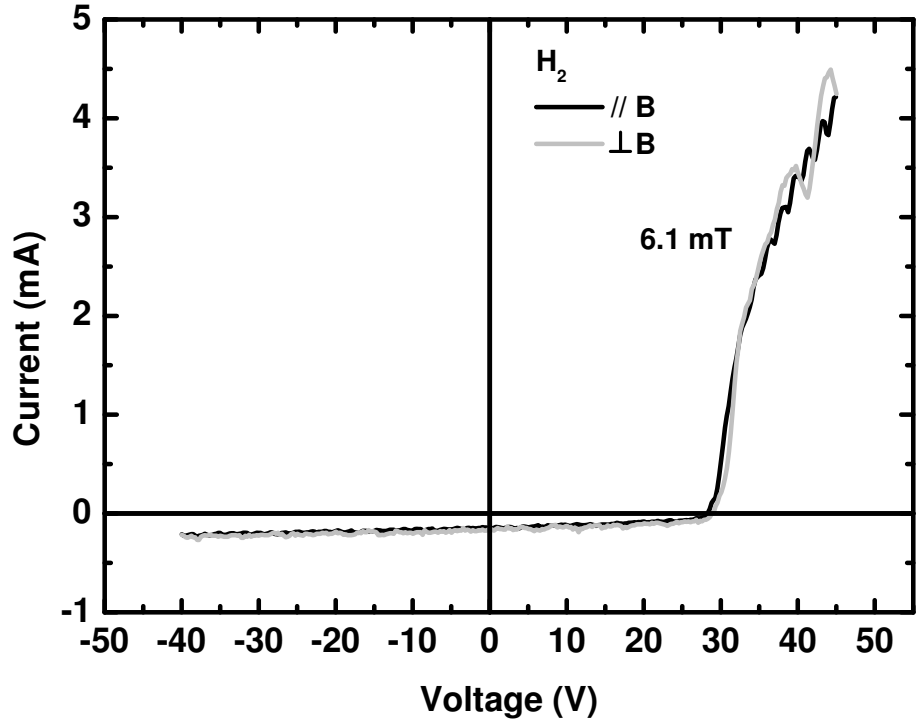

Figure 4. IV curves recorded in the position 3 for the horizontal and 5 for the vertical probe and a magnetic field of 6.1 mT.

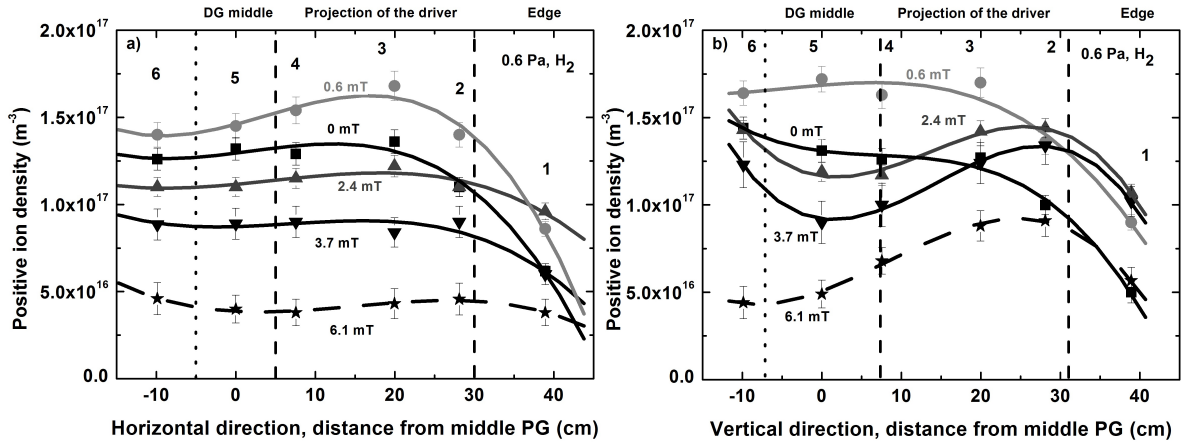

Figure 5. a) and b) present the positive ion density variation in the horizontal and vertical direction in hydrogen for different magnetic field strength and the no field case. The results were obtained for 0.6 Pa discharge pressure and a total injected RF power of 160 kW. The labels are corresponding to the ones on figure 2.

ever, not encountered at RADI where the plasma could be sustained at 0.2 Pa with a strong magnetic field inside the driver, probably because of its larger driver size, the different 3D map of the magnetic field, and the higher gas flow required for operation

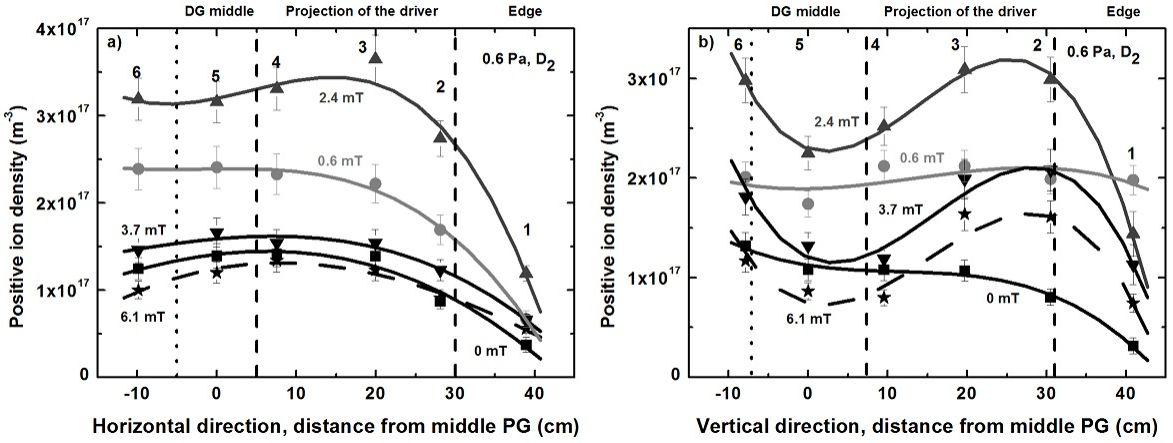

Figure 6. a) and b) present the positive ion density variation in the horizontal and vertical direction in deuterium for different magnetic field strength and the no field case. The results were obtained for 0.6 Pa discharge pressure and a total injected RF power of 160 kW. The labels are corresponding to the ones on figure 2.

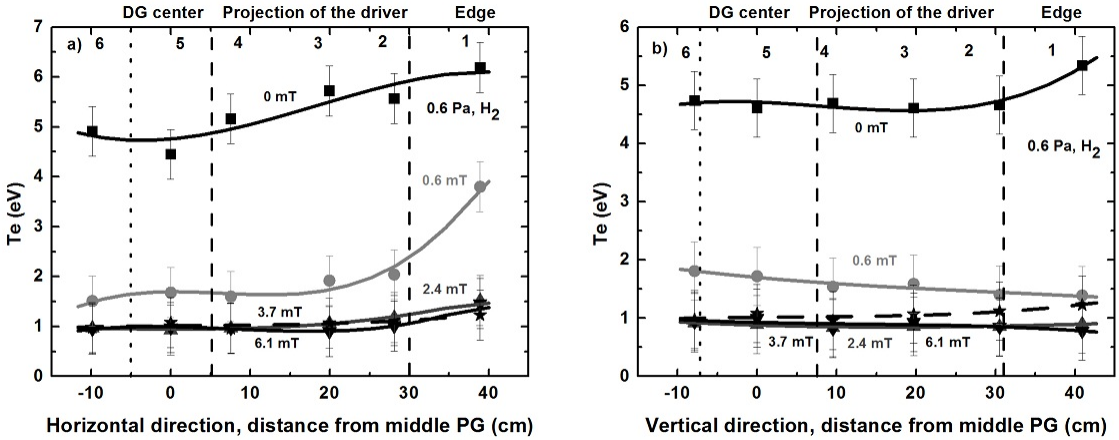

Figure 7. a) and b) present the electron temperature variation in the horizontal and vertical direction in hydrogen for different magnetic field strength and the no field case. The results were obtained for 0.6 Pa discharge pressure and a total injected RF power of 160 kW. The labels are corresponding to the ones on figure 2.

at low filling pressure.

In order to enhance the conversion of neutrals and positive ions into negative ions on the plasma grid, the evaporation of caesium is mandatory as it reduces the work function of the surfaces [8, 20, 22, 23, 24]. However, due to an overlapping of caesium and magnetic field influences on the plasma homogeneity, no caesium was evaporated at RADI. The magnetic field was generated by a current (up to 5 kA) flowing through the dummy grid. In contrast to [4] where the magnetic field intensity was lower for the same current flowing into the dummy grid, the DG current returning conductors are now fixed near the drivers. With this configuration, the intensity of the magnetic field is strengthened. The return lines close to the driver also lowers the field in the downstream region, which

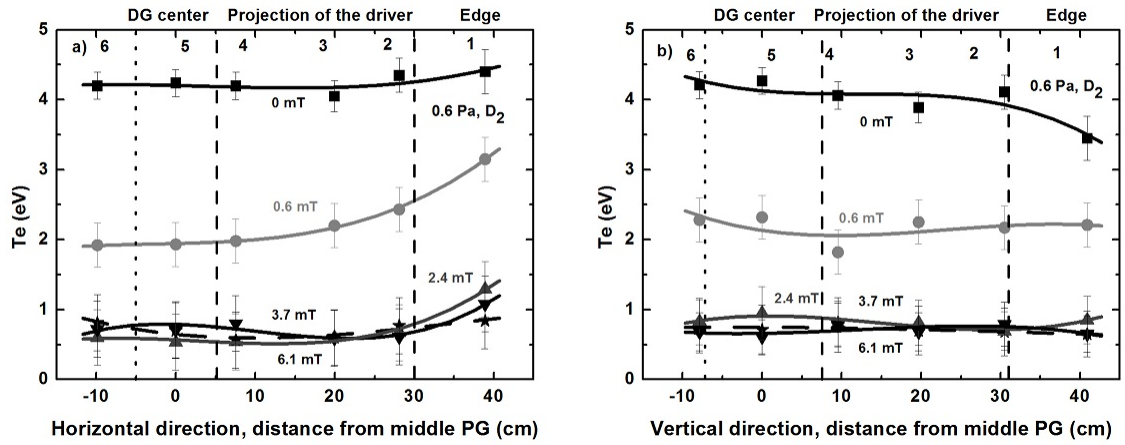

Figure 8. a) and b) present the electron temperature variation in the horizontal and vertical direction in deuterium for different magnetic field strength and the no field case. The results were obtained for 0.6 Pa discharge pressure and a total injected RF power of 160 kW. The labels are corresponding to the ones on figure 2.

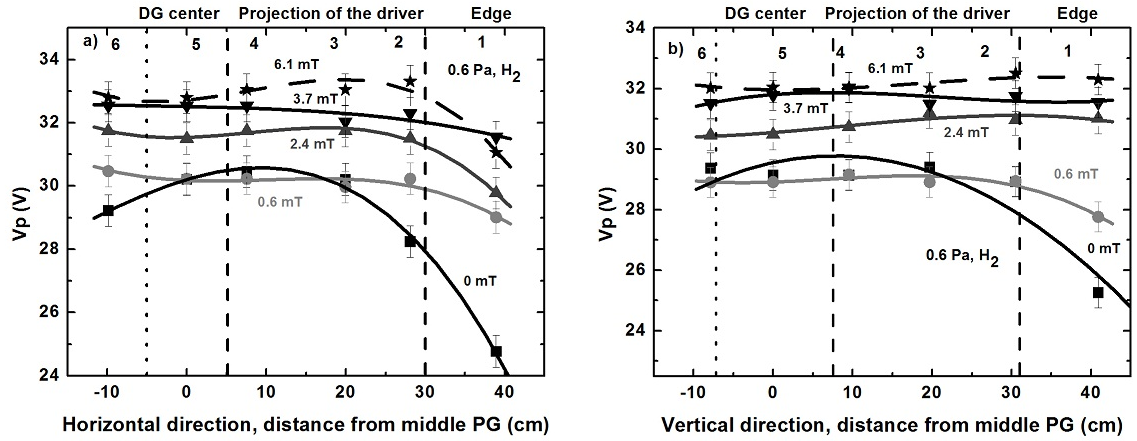

Figure 9. a) and b) present the plasma potential variation in the horizontal and vertical direction in hydrogen for different magnetic field strength and the no field case. The results were obtained for 0.6 Pa discharge pressure and a total injected RF power of 160 kW. The labels are corresponding to the ones on figure 2.

is advantageous for beam extraction. For these experiments, the magnetic field intensity in front of the grid linearly varies from 0.6 mT at 0.5 kA up to 6.1 mT at 5 kA. Figure 2a shows a 2D map representation of the magnetic field for a 5 kA current flowing in the dummy grid. Figure 2b shows the variation of the horizontal magnetic field intensity along the direction indicated by the arrow seen on figure 2a. As can be seen on figure 2a, the magnetic field shows a more or less homogeneous profile with a strength of about 6.1 mT in front of the grid (the field topology is independant of the current).

Two Langmuir probes were were used during this study: a vertical and a horizontal probe, both at a distance of 2 cm from the grid. The probe tip dimensions are 125 μm

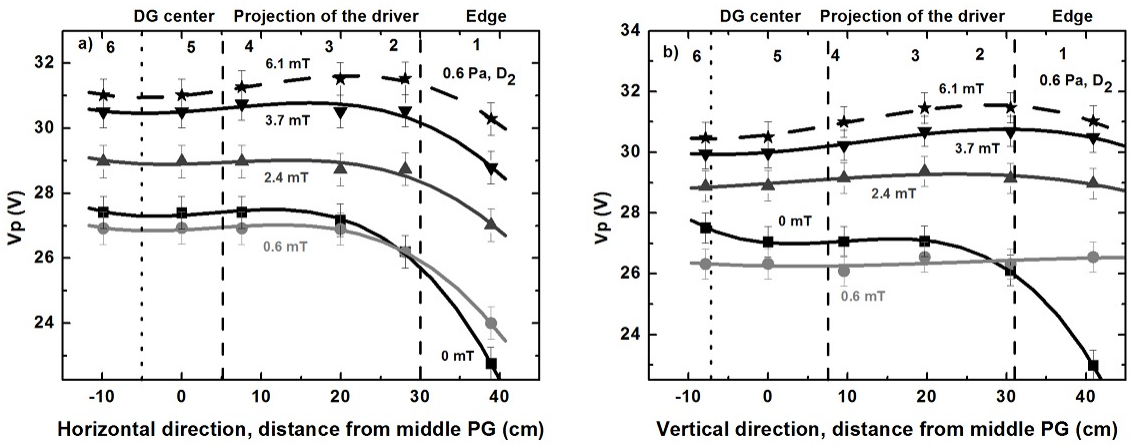

Figure 10. a) and b) present the plasma potential variation in the horizontal and vertical direction in deuterium for different magnetic field strength and the no field case. The results were obtained for 0.6 Pa discharge pressure and a total injected RF power of 160 kW. The labels are corresponding to the ones on figure 2.

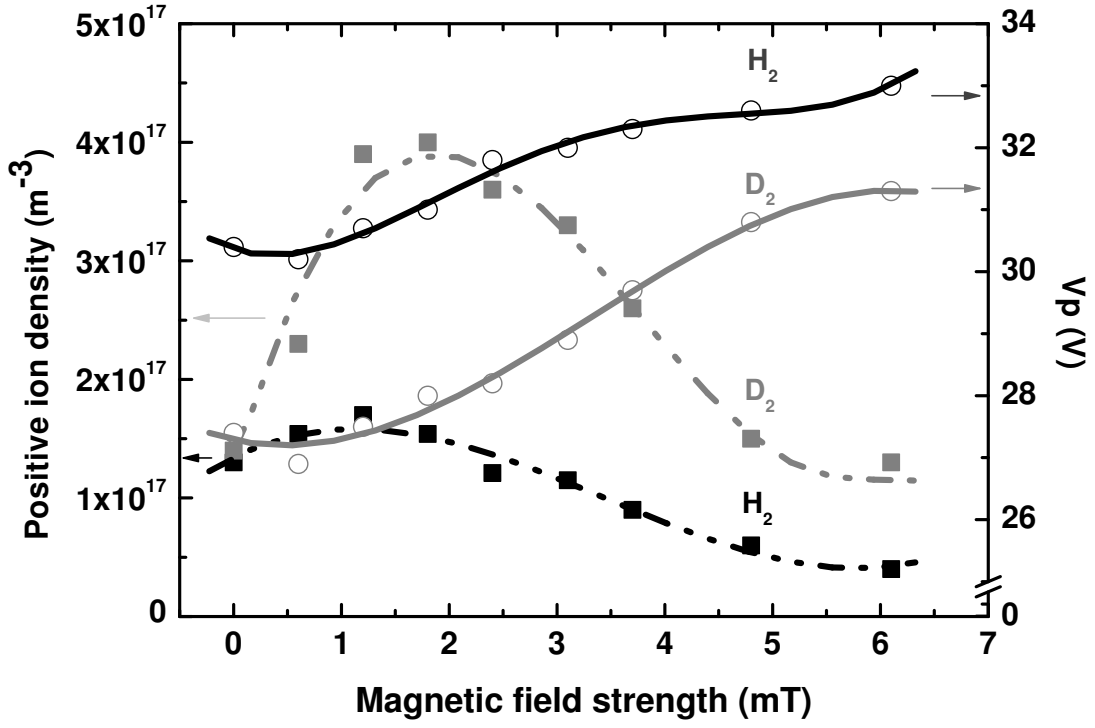

Figure 11. Evolution of the positive ion density and the plasma potential in hydrogen and deuterium discharges as a function of the magnetic field strength in front of the grid.

radius and 0.5 cm long. The probes are RF compensated. The analysis system is the PlasmaMeter developed at the School of Physics and Technology of the K.N. Karazin

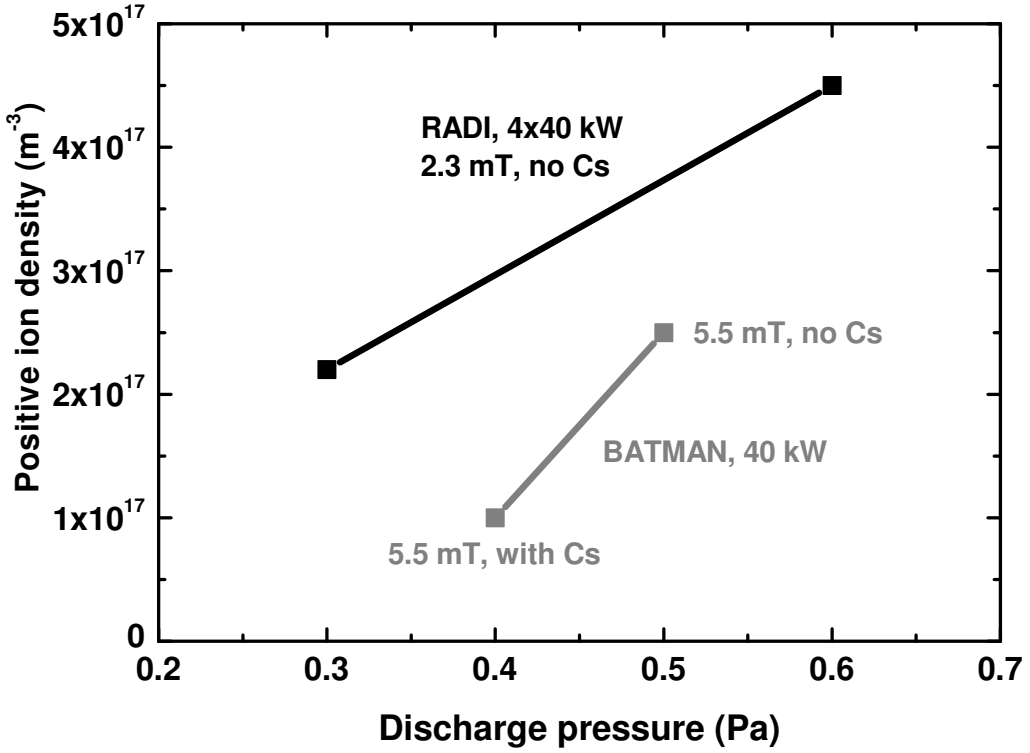

Figure 12. RF efficiency, BATMAN / RADI comparison.

Kharkov National University, Ukraine [25]. Figure 3 shows the probe arrangement and the locations chosen for the measurements. The labels on figure 3 are the measurement positions. The magnetic field configuration is such that the horizontal and vertical probe tips are parallel and perpendicular to the magnetic field lines respectively.

The plasma potential was evaluated at the zero-crossing of the second derivative of the I-V curve of the probe. For all the measurements, the zero-crossing point of the second derivative was well defined and the difference between the maximum and the minimum of the second derivative was lower than kT_e/e. Typically, kT_e/e was in the order of 1 V. The electron temperature was evaluated by a linear approximation of the logarithm of the second derivative. For high electron temperature (no magnetic field) the error is small. When increasing the magnetic field strength, the plasma density and electron temperature decrease. Due to a lower signal to noise ratio the error is larger, ΔTe= 0.5 eV. The ion saturation current was taken at a potential of Vp-10kT_e for each measurement. At such potential, the contribution of the high energy electrons to the current is negligible. The systematic error in the probe current measurement is roughly $\pm 20\mu$A. The accuracy in the ion density evaluation is limited by the knowledge of the exact ion mass, a direct measurement of the proportion of each ion species (H^+, H_2^+ and H_3^+)

being not possible. In principle, the ion mass vary between 1 and 3. An estimation of the effective mass can be done provided the measurements of the species distribution for positive H ion beams extracted from other RF sources. Pressure and RF power scan were performed at a source [26] (functionally identical to the drivers of the ion source used in this study) operated for the decomissioned W7-AS stellerator. Results found a proportion of 40% H^+, 40% H_2^+ and 20% H_3^+ resulting in 1.8 being the most probable effective mass. Due to the low electronegativity of the plasma (less than 10 % without caesium [27]), the influence of the negative ions on the I-V curve can be neglected. The influence of the magnetic field on the probe traces is discussed in the next section. In the following the variation of the positive ion density, electron temperature and plama potential profiles will be presented, followed by a comparison of the RF efficiency of the BATMAN and RADI test beds.

3. Results and discussion

The horizontal and vertical probe tips being parallel and perpendicular to the magnetic field lines respectively, the influence of the magnetic field on the collection of charged species by the probes could be investigated. It is known that a magnetic field can reduce the electron current collected by the probe due to the electrons following the magnetic field lines [28]. For a typical cylindrical probe, the following inequality must be statisfied for the fulfilment of the small-probe assumption [29]:

$$a\, ln\left[\frac{\pi l}{4a}\right], \lambda_d \ll inf(\lambda_e, r_l) \tag{1}$$

Here, a is the probe radius, l the probe length, λ_d the Debye length and *inf*(λ_e,r_l) is the smaller of the electron mean free path λ_e or the Larmor radius r_l. For T_e = 1 eV, $n_e = 10^{17}\,cm^{-3}$ and B = 6.1 mT (value of the maximum achievable magnetic field strength) the electron gyroradius (600 μm) is greater than both the criterion given by eq. 1 (400 μm) and the Debye length (23 μm). The comparison between the gyro radius and the eq. 1 criterion is however not fully satisfied for a field of 6.1 mT. In order to determine whether or not the magnetic field had a noticeable influence on the electron branch of the probes traces, the Langmuir probes were parked at position 3 for the horizontal probe and at position 5 for the vertical probe (see figure 3). Figure 4 shows that for a magnetic field of 6.1 mT, a difference can be observed in the electron branch, but it is small enough to be neglected. It results only in an increase in the size of the error bars.

Figures 5a and b, 6a and b, present the positive ion density in both the horizontal and vertical direction, for different magnetic field strengths and for 0.6 Pa, 80 kW per generator (40 kW per driver) in both hydrogen and deuterium discharges respectively. As can be seen on figures 5a and 6a, aside from a decay of the plasma near the source walls, the plasma is homogeneous (within 10 %) in the horizontal direction in hydrogen and deuterium, whatever the magnetic field strength. In the vertical direction the plasma is

homogeneous only for the no- and low-field cases (0.6 mT) as can be seen on figures 5b and 6b for hydrogen and deuterium respectively. For a magnetic field strength higher than 2.4 mT a minimum appears between 0 and 20 cm, on figures 5b and 6b. This density drop occurs between the drivers.

In the smaller testbed BATMAN, a difference between top and bottom parts of the plasma grid (an order of magnitude difference between the top and bottom currents) was observed and is due to cross-B drifts [8, 12, 30]. At RADI, a decay to the edges was observed with the previous magnetic field configuration [5]. The presence of cross-B drifts was also expected at RADI because of the magnetic field. However, from what can be seen on figures 5 and 6, at RADI, only a decrease between the drivers is observed in the vertical direction (see figures 5b and 6b). This decrease between the drivers could be also due to cross B drifts, however the difference in the measured currents is much lower than what was observed at BATMAN. A possible explanation for this dip between the drivers could be due to the diffusion coefficient perpendicular to the magnetic field being smaller, contrary to parallel diffusion which remains unaffected by the magnetic field. Consequently, the strong gradients observed at BATMAN and the small dip seen at RADI seems to originate from different mechanisms: cross B drifts in the case of BATMAN, while a smaller diffusion at RADI may explain the observations. As a consequence, the size of the drivers at ELISE was changed to be larger than those used for RADI, so as to reduce the magnitude of the dip by overlapping the plasmas flowing out of each drivers. Moreover, it has been observed at RADI that a better homogeneity was achieved with a lower discharge pressure [5]. The dip vanishes at 0.3 Pa which is the relevant operating pressure of the ITER NNBI sources.

When compared to BATMAN, the larger size of the RADI testbed as well as the use of four drivers instead of one, can also contribute to the better homogeneity achieved in front of the grid because of the overlapping of the plasmas flowing out of each driver. From these measurements one can see that the plasma density in the vertical and horizontal directions are comparable for the low field cases both in H and D. It can also be seen that the positive ion density achieved in deuterium is higher than in hydrogen. On figures 5 and 6, it can be observed that a strong magnetic field results in a lower observed density, which will be discussed below. The grid illumination by the positive ions and electrons (not shown here) is homogeneous in the horizontal direction while a decrease between the drivers (50%) is observed in the vertical direction.

The figures 7a, b and 8a and b show the hydrogen and deuterium electron temperatures respectively. The same trends and values were measured in hydrogen and deuterium. An electron temperature between 4 and 6 eV is found without magnetic field in hydrogen and deuterium. Neglecting the data near the source walls, an overall good homogeneity to within 10% was obtained. As can be seen on the figures, even a weak magnetic field of 0.6 mT strongly decreases the electron temperature to below 2 eV in hydrogen and to below 3 eV in deuterium. A field of 2.4 mT, is needed for both isotopes, to decrease the temperature to 1 eV. When the electron temperature is below 2 eV, the stripping of negative ions by electrons becomes negligible and the dominant negative ion destruction

mechanism becomes the mutual neutralization with positive ions. Even with a magnetic field higher than 2.4 mT it is not possible to further decrease the electron temperature. The results at BATMAN shows an electron temperature in front of the PG comprised between 1 and 2 eV [12]. The new results for RADI show that despite the larger size of RADI when compared to BATMAN, as well as the different magnetic field configuration and the way it is generated, comparable electron temperatures can be achieved in front of the grid.
The potential profiles are presented on figures 9a, b and 10a and b. Besides the decay to the walls, an overall good homogeneity is found. The increase of the plasma potential with the filter field strength combined with a decrease of the electron temperature and the positive ion density can be interpreted as an increased losses to the walls. For a field strength of 0.6 mT, the electron gyration frenquency is in the order of 1.7x10^7 Hz, while the total electron collision frequency (with neutrals, H^+, H_2^+ and H_3^+ ions) is of 5.0x10^6 Hz [31]. As a consequence, whatever the field strength is, the electrons are magnetized and follow the magnetic field lines. As can be seen on figure 2a, these field lines intercept the walls. The plasma potential is higher at RADI when compared to BATMAN [12]. Two aspects explain this difference. First, it has been observed at BATMAN that the plasma potential was strongly affected by the presence of Cs [32, 33]. Second, the difference probably lies in the magnetic field configuration and to the surface to volume ratio of each test bed.

Despite that only a fraction of the plasma parameters in the neighbourhood of the dummy grid could be obtained due to the Langmuir probe hardware restrictions, the results shown in figures 5 to 7 indicate that the homogeneity achieved on large sources is significantly higher than the one obtained on smaller testbeds. In figures 6a and 6b of ref [8], one can see that saturation currents, plasma potentials and temperatures obtained at BATMAN strongly differ between top and bottom, because of the presence of cross-B drifts. The larger size of RADI and the use of four drivers seems to reduce the influence of these drifts leading to an overall better homogeneity of the plasma parameters, which is favorable for ITER sources.

In order to better illustratre the behaviour of the plasma parameters with the magnetic field strength, figure 11 shows the variation of the plasma potential and the positive ion density with the magnetic field strength in front of the DG for the x = 7.55 cm position (corresponding to the measurement number 4 in the horizontal direction). One can clearly see that in hydrogen, a maximum in the density is achieved around 1 mT, while in deuterium a maximum in the density is achieved at around 2 mT. In both hydrogen and deuterium, when compared to the no field case, one observes that the plasma potential does not increase at 0.6 mT. At 0.6 mT in hydrogen, this field strength corresponds roughly to the maximum of density in hydrogen. In deuterium the maximum in density is achieved for a field strength of 2 mT and the plasma potential has only increased by 0.5 V as compared to the no field case. For hydrogen and deuterium, the electron

temperature decreased to below 2 eV for either the 0.6 mT or 2 mT field as compared to the no magnetic field case (see figures 7a and 8a). For weak field cases, one observes a decrease of the electron temperature and a slight decrease in the diffusion, leading to a reduction of the losses to the walls. It can then be concluded from the combination of: a stable plasma potential, a decrease of the electron temperature, and a peaked density profile that a form of enhanced confinment is achieved for low magnetic field strength. For higher field strength, the electron temperature remains constant (see figures 7 and 8), while the electrons are becoming more and more strongly magnetized with the increase of the magnetic field. It is likely that transport to the side walls more losses occurs on the side walls increases, leading to a higher plasma potential and a reduction of the density as can be seen on figure 11.

On ELISE as well as on SPIDER, the size of the sources will be larger than the ones on RADI (+10 cm at each side) in order to reduce the decay of the plasma to the walls inside of the projection of the driver. The diameter of the drivers will also be larger (30 cm instead of 24 cm). Two favorable effects are then expected to be achieved. First, the operating pressure of larger sources can be as low as 0.2 Pa in the presence of a magnetic field as was shown at RADI. Second, the RF efficiency (density achieved at a certain pressure and power) of the RADI and BATMAN test facilities should differ. A comparison is made on figure 12, of the highest positive ion densities achieved in front of the grid, with an electron temperature lower than two electron-volts, regardless of the magnetic field strength. The measurements were taken at a distance of 2 cm of the grid in each case. It appears that with the higher flexibility of the magnetic field at RADI, a higher density can be achieved at the same injected power and pressure. Moreover the larger volume to surface ratio of RADI can also be resposible to reduced losses. One can then expect that for the large test beds, the same amount of negative ions will be extracted with a smaller injected RF power, which mitigates the risks of high RF power operation (arcs) and gives more experimental flexibility when compared to small test beds. The higher RF efficiency should result in a larger amount of extracted negative ions due to an increase of the positive ion flux and neutrals onto the grid as was shown in [34].

4. Conclusion

Investigations were performed in order to determine the homogeneity of the plasma parameters in front of dummy grid of the source on the RADI test bed. Besides its increased size, the main difference between RADI and the other test beds devoted to the optimisation of negative ions source for ITER NBH is the way the magnetic field is generated near the grid. At RADI, a current flowing through the grid generates the magnetic field, while permanent magnets are used on the other test beds equipped with small prototype sources. The Langmuir probe configuration at RADI permitted the determiation of the influence of a magnetic field on the collection of charged species

by Langmuir probes. Up to a field strength of 6.1 mT no difference was observed up to between probes whose tip was parallel and perpendicular to the field lines. Langmuir probe measurements showed that all the plasma parameters were homogeneous to within 10 % in the direction parallel to the magnetic field. In the direction perpendicular to the magnetic field, a dip in the positive ion density wasfasym observed between the drivers at 0.6 Pa, for a magnetic field strength higher than 2 mT, the other plasma parameters remaining homogeneous. This decrease in the density was attributed to the lower diffusion of charged species across a perpendicular magnetic field. This study shows that the grid illumination in large sources, as well as the other plasma parameters are significantly more homogeneous than in smaller test beds. This study also showed that an electron tempereture of 1 eV could be easily achieved, which is important to minimize the destruction of the negative ions by electron collisions. A type of enhanced confinement is achieved for low magnetic field strength. Finally, a comparison of the RF efficiency showed that for the same injected power and pressure, the larger volume to surface ratio of RADI when compared to BATMAN resulted in a higher density in front of the grid. Morevover, a greater flexibility for the RF power management, as well as a risk mitigation is foreseen for the large sources ELISE and the ITER-like source SPIDER due to the larger RF effieciency.

5. Acknowledgements

The work was supported by a grant from Fusion for Energy (F4E GRT-313) supervised by Antonio Masiello. The opinions expressed herein are those of the authors only and do not represent the Fusion for Energy's official position.

6. References

[1] Speth E. et al., Nucl. Fus. 46 (2006) 220.
[2] Franzen P. et al., Nucl. Fus. 47 (2007) 264.
[3] Heinemann B. et al., Fus. Eng. and Des. 84 (2009) 915.
[4] Franzen P. et al., Fus. Eng. and Des. 82 (2007) 407.
[5] Fantz U. et al., AIP Conf. Proc. 1097 (2009) 265.
[6] Schiesko L. et al., Nucl. Fusion 51 (2011) 113021.
[7] Kraus W. et al., Rev. Sci. Inst. 79 (2008) 02C108.
[8] Schiesko L. et al., Plas. Phys. & Cont. Fus.53 (2011) 085029.
[9] Franzen P. Plasma Phys. Control. Fusion 53 (2011) 115006.
[10] Sonato P. al., Fusion Eng. Des. 84 (2009) 269.
[11] Singh M. J. and De Esch H. P. L., Rev. Sci. Inst. 81 (2010) 013305.
[12] Schiesko L. et al., Plas. Phys. & Cont. Fus. 54 (2012) 105002.
[13] Fantz U. et al, Nucl. Fusion 49 (2009) 125007.
[14] Franzen P et al, AIP Conf. Proc. 1390 (2010) 310.
[15] Kolev St. et al., Plas. Phys. & Cont. Fus. 49 (2007) 1349.
[16] Boeuf J.-P. et al. *Plasma Sources Sci. Tech.*, 20 (2011) 015002.
[17] Taccogna F. et al. *Plasma Sources Sci. Tech.*, 20 (2011) 024009.
[18] Mochalskyy S. *J. App. Phys.*, 111 (2012) 113303.
[19] Fubiani G. *Phys. Plas.*, 19 (2012) 043506.
[20] Lee B. S. and Seidl M. *Appl. Phys. Lett.*, 61 (1992) 2857.
[21] McNeely P and Wünderlich D. *Plasma Sources Sci. Tech.* 20 (2011) 045005.
[22] Isenberg J. D., Kwon H. J., and Seidl M. *AIP Conference Proceeding*, 287 (1994) 38.
[23] Simonin A. et al. *Rev. Sci. Instrum*, 67 (1996) 1102 .
[24] Gutser R. et al., Rev. Sci. Inst 82 (2011) 023506.
[25] McNeely P., Dudin S. V., Christ-Koch S., Fantz U. and NNBI Team, Plas. Sources Sci. and Technol., 18 (2009) 014001.
[26] Rust N. et al. *Fus. Eng and Cont. Fusion (Montreux, Switzerland, 17-21 June 2002)*, published on CD-ROM.
[27] Berger M., Fantz U., Christ-Koch S. and NNBI Team, Plas. Sources Sci. and Technol., 18 (2009) 025004.
[28] Laframboise J. G. and Rubinstein J., Phys. Fluids, 19 (1976) 12
[29] Godyak V. A. and Demidov V. I., J. Phys. D, 44 (2011) 233001.
[30] McNeely P. and Schiesko L., Rev. Sci. Inst., 81 (2010) 02B111.
[31] Wuenderlich D., private communication.
[32] Schiesko L., To be published.
[33] Fantz U. et al., Plas. Phys. & Cont. Fus. 49 (2007) B563.
[34] Wuenderlich D., Gutser R. and Fantz U., Plasma Sources Sci. Technol. 18 (2009) 045031